

**$\beta$ -delayed proton decay of  $^{29}\text{S}$** 

D. J. Vieira, R. A. Gough, and Joseph Cerny

*Department of Chemistry and Lawrence Berkeley Laboratory, University of California, Berkeley, California 94720*

(Received 30 May 1978)

The  $^{28}\text{Si}(^3\text{He}, 2n)$  reaction at 32 MeV has been used to produce  $^{29}\text{S}$ ; delayed protons have been observed following the positron decay of  $^{29}\text{S}$  to proton unbound levels in  $^{29}\text{P}$ . The half-life of  $^{29}\text{S}$  was measured to be  $187 \pm 6$  ms which, combined with previous results, gives a weighted average value of  $188.0 \pm 4.3$  ms. Precise level energies have confirmed several recently observed states in  $^{29}\text{P}$  from 4.0 to 9.5 MeV in excitation energy. From the intensities of these proton groups and assuming isospin purity for the lowest  $T = 3/2$  level in  $^{29}\text{P}$ , absolute  $\log ft$  values for each transition were determined. The measured excitation energies and  $\beta$  decay transition rates to levels in  $^{29}\text{P}$  are compared to recent shell-model calculations.

[RADIOACTIVITY  $^{29}\text{S}$ ; measured  $\beta$ -delayed protons, measured  $T_{1/2}$ ;  $^{29}\text{P}$  deduced levels, IAS proton decay, deduced  $\log ft$  values compared to shell model.]

## I. INTRODUCTION

The nuclide  $^{29}\text{S}$  is a relatively uninvestigated member of the  $T_z = -\frac{3}{2}$ ,  $A = 4n + 1$  series of strong  $\beta^+$ -delayed proton precursors.<sup>1</sup> The decay schemes of these nuclei are characterized by strong branching (12–100%) to unbound levels in the daughter nuclei which subsequently break up by emitting protons of discrete energies. By accurately measuring the energies and intensities of these delayed protons, it is possible to determine excitation energies of states in the daughter nucleus and further to determine the  $\beta$  decay transition strengths feeding them. Such spectroscopic studies of the  $\beta^+$ -delayed proton decay of  $^{29}\text{S}$  are presented herein.

Shell-model calculations in the  $2s1d$  shell have proved to be quite successful in predicting energy levels, spectroscopic factors for single nucleon transfer reactions, and transition rates for  $\beta$  and  $\gamma$  decay. Chung and Wildenthal<sup>2</sup> have recently performed shell-model calculations employing a large basis space for the mass 29 system. Comparison of these predictions with experimental excitation energies and  $\beta^+$ -transition rates from the decay of  $^{29}\text{S}$  to levels in  $^{29}\text{P}$  provides a most challenging test for such calculations since this nuclide is located essentially in the middle of the shell.

Although  $\beta^+$ -delayed proton decay of  $^{29}\text{S}$  has been observed previously,<sup>3,4</sup> these earlier experiments were hindered by large background produced primarily by multiply-scattered electrons, as well as by poor energy resolution. In the present experiment good energy resolution, low background delayed proton spectra covering an energy region from 700 keV to 8 MeV have been obtained using counter telescopes and particle identification techniques in conjunction with a He-jet transport system. More than fifteen previously unobserved delayed proton groups have been characterized.

## II. EXPERIMENTAL PROCEDURE

The  $^{28}\text{Si}(^3\text{He}, 2n)$  reaction was utilized to produce  $^{29}\text{S}$  in irradiations of natural silicon targets with the 32 MeV  $^3\text{He}$  beam of the Lawrence Berkeley Laboratory 88-in. cyclotron. After degrading through an isolation foil and helium (see below), the incident beam energy on target was 31.3 MeV which is expected to be near the maximum for producing  $^{29}\text{S}$  and still below the threshold of the competing ( $^3\text{He}, \alpha 2n$ ) reaction at 32.1 MeV which would produce the next lighter member in this series,  $^{25}\text{Si}$ . Use of the He-jet system permitted fast transport of the produced activity to a low background area where studies employing good energy resolution were performed. Since this system has been described previously,<sup>5,6</sup> only a brief discussion will be given here.

Silicon targets of  $600 \mu\text{g}/\text{cm}^2$  in thickness located in a chamber pressurized with He to 1200 Torr were bombarded by the  $^3\text{He}$  beam after entry through a  $5.1 \mu\text{m}$  nickel isolation foil. Reaction products which recoiled out of the target and thermalized in the helium gas were transported through a 40 cm long stainless steel capillary tube to a counting chamber which was maintained at a pressure of 0.15 Torr by a high capacity Roots-blower mechanical pump. Transported activity was deposited on aluminum foils mounted on a flipper wheel which rotated sequentially in  $60^\circ$  steps, positioning the collected activity in front of a counter telescope. Collection and counting of activity on adjacent foils took place simultaneously so that no pulsing of the beam was required. The detector geometry was such that only activity originating from the foil at the counting station was detectable, precluding any activity at the collection station from being observed. To increase

the overall transport/collection efficiency (by as much as an order of magnitude) a small amount of air (1–5%) was added to the helium carrier gas and the mixture was subsequently bubbled through a solution of ethylene glycol. This improvement presumably arises from aerosol/cluster formation which is known<sup>7</sup> to be important for efficient transport in such systems.

Several  $\Delta E$ - $E$  counter telescopes consisting of phosphorus diffused silicon and surface barrier detectors of various thicknesses were used to span the broad energy region necessary to cover all significant proton decays. Low energy delayed protons were studied with a telescope consisting of a 6.3  $\mu\text{m}$   $\Delta E$  detector and a 94  $\mu\text{m}$   $E$  detector, while a 29  $\mu\text{m}$   $\Delta E$ -508  $\mu\text{m}$   $E$  telescope was employed to detect protons with energies up to 8 MeV. Other detector combinations were also used to overlap the intermediate energy region. All of these counter telescopes subtended a solid angle of 0.24 sr and were followed by a large area detector which rejected any long range particles traversing the telescope. To reduce noise in the detectors and to improve their timing characteristics, all detectors except the 6.3  $\mu\text{m}$  detector were thermoelectrically cooled to  $-15^\circ\text{C}$ .

Those  $\Delta E$ - $E$  events which met a fast coincidence requirement ( $2\tau \approx 40$  ns) and which identified as protons were stored in eight time-routed, 512 channel spectra. The first spectrum covered events observed during the first 50 ms of the counting period, while the remaining seven spectra corresponded to sequential 65 msec counting intervals. Data acquired in this fashion provided half-life information for each significant proton group. Unrouted energy spectra were also accumulated in a 2048 channel analyzer. Finally, individual pro-

ton groups or selected energy regions were stored on a 400 channel multiscalar which was advanced by a precise quartz-crystal oscillator for supplementary half-life information.

### III. EXPERIMENTAL RESULTS

#### A. Proton spectra

Two of the delayed proton spectra obtained from these  $^3\text{He}$  bombardments are shown in Figs. 1 and 2. Figure 1 represents data accumulated in 150 000  $\mu\text{C}$  of integrated beam using a detector telescope which allowed protons to be reliably identified from 1.8 to 8.0 MeV. The proton spectrum shown in Fig. 2 was obtained with a lower energy telescope (energy span 0.7 to 2.8 MeV) in 94 000  $\mu\text{C}$  of integrated beam. Additional data, not shown here, were also acquired and incorporated into the following analysis and calculations.

All the proton groups labeled with numbers are attributed to delayed protons from  $^{29}\text{S}$  produced by the  $^{28}\text{Si}(^3\text{He}, 2n)^{29}\text{S}$  reaction, which has a threshold energy of 21.6 MeV (all masses are taken from Ref. 8 unless otherwise stated). These assigned peaks exhibit the same half-life to within their respective uncertainties. No other known delayed proton precursors can be produced at this bombarding energy from pure silicon targets or from the nickel entrance foil. Delayed protons from  $^{13}\text{O}$  and  $^{17}\text{Ne}$  could be produced from the carbon or oxygen present in the He-jet additives (ethylene glycol and air), but since these precursors are gases, little activity is expected to "stick" to the collection foil and no evidence of delayed protons arising from either nuclide was observed. However, two contaminant groups were

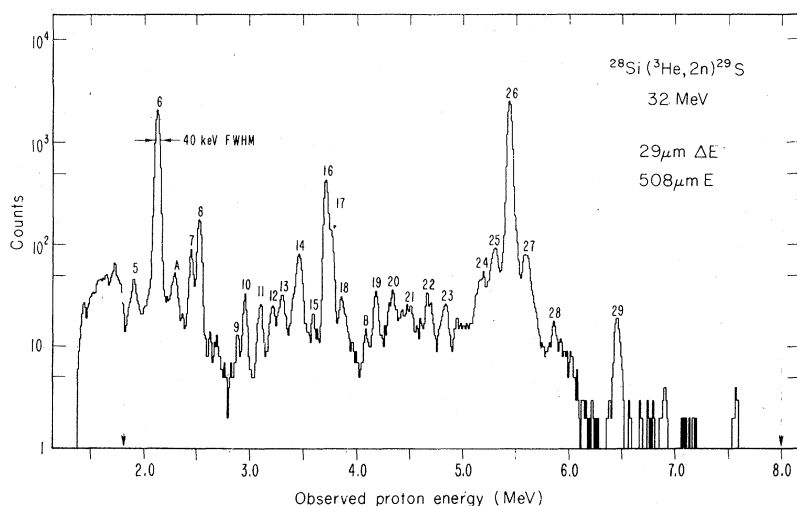


FIG. 1. The proton spectrum observed following the  $\beta^+$  decay of  $^{29}\text{S}$  to unbound levels in  $^{29}\text{P}$ . All numbered peaks are identified with the decay of  $^{29}\text{S}$  (groups A and B arise from contaminants). The dashed vertical arrows indicate the energy region over which protons could be reliably identified.

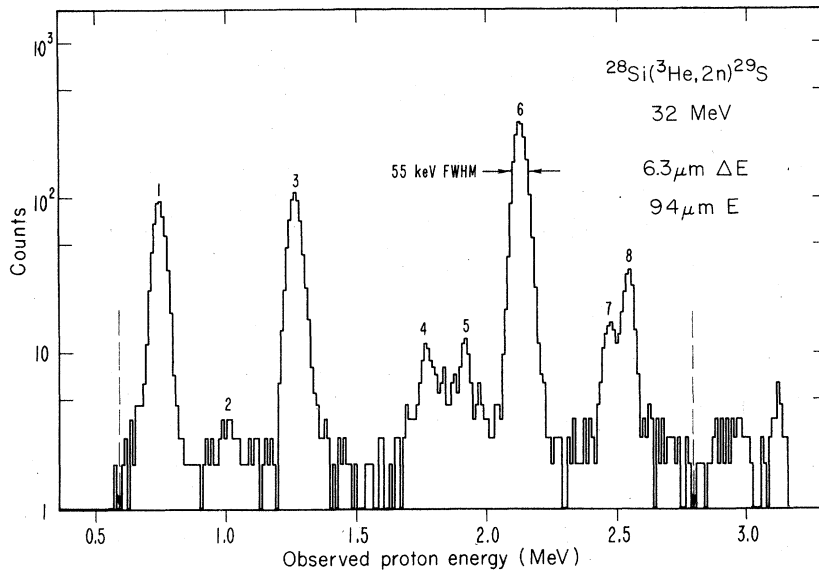


FIG. 2. Delayed protons from  $^{29}\text{S}$  with energies less than 2.8 MeV. As in Fig. 1, the dashed vertical arrows indicate the energy region over which protons could be reliably identified.

observed and are labeled with letters. Group A was observed *only* in the data shown in Fig. 1. No evidence for this group can be seen in Fig. 2 or in any of the other data that were obtained. The origin of this group is uncertain, but it definitely does *not* originate from the decay of  $^{29}\text{S}$ . Peak B is attributed to the decay of  $^{25}\text{Si}$  since its energy coincides with the energy of the strongest delayed proton group<sup>6</sup> of  $^{25}\text{Si}$ ; the relative intensity of this group was observed to vary widely from target to target, which is consistent with its arising from the  $(^3\text{He}, 2n)$  reaction on a small magnesium contamination (<0.2%) present in some of the silicon targets.

As a further check for unknown contaminants present in the He-jet system, a pulsed beam experiment was performed in which reaction products retained in the target were detected by a counter telescope protected by a slotted rotating wheel system.<sup>9,10</sup> Results from this latter experiment, which were performed in vacuum, needing no entrance foil, were in total agreement with the assignments shown above.

A search for low energy protons with energies less than 700 keV was performed by observing events in a well-collimated  $14\ \mu\text{m}\ \Delta E$  detector which was followed by a  $260\ \mu\text{m}\ E$  detector with the latter placed in anticoincidence. No other significant groups with energies greater than 350 keV were observed.<sup>10</sup>

#### B. Energy measurements

Energy calibration was obtained using the well-known energies<sup>6</sup> of delayed protons originating from  $^{25}\text{Si}$  produced in  $^3\text{He}$  bombardments of mag-

nesium targets. Further calibrants came from several of the large groups observed in the data which arise from the decay of accurately known levels in  $^{29}\text{P}$ . In particular, group 6 is attributed to the proton decay of a state at 4.954 MeV (Ref. 11) (see Table I), while groups 1 and 7 arise from the breakup of a state at 5.293 MeV (Ref. 11) to the first excited state and ground state of  $^{28}\text{Si}$ , respectively. Similarly, proton decay of the lowest  $T = \frac{3}{2}$  state in  $^{29}\text{P}$  at 8.381 MeV to the first excited state and ground state of  $^{28}\text{Si}$  results in proton groups 16 and 26. The excitation energy of this state and its corresponding proton decay energies represent a weighted average of proton resonance,<sup>12,13</sup>  $\gamma$  decay,<sup>14,15</sup> and  $\beta$  delayed proton<sup>16</sup> data where the most accurate proton separation energy<sup>11</sup> for  $^{29}\text{P}$  has been incorporated. Using these as calibrants, the energy of each group was extracted from their observed centroid, which after correcting to the center-of-mass system, resulted in the final proton energies given in Table I.

#### C. Half-life measurements

Half-lives were obtained from seven point decay curves for each observed group (the first time group was discarded since it partially overlapped with the settling time of the flipper wheel). Further half-life determinations were obtained from data taken with the multiscalar. Both methods gave consistent results. Background was reduced to a negligible level by particle identification and in no case was a two component fit necessary. A half-life of  $187 \pm 6$  ms for  $^{29}\text{S}$  was obtained from four independent measurements. This agrees

TABLE I. Observed proton energies from the decay of unbound levels in  $^{23}\text{P}$  (fed by the  $\beta^+$  decay of  $^{23}\text{Si}$ ) to various final states in  $^{23}\text{Si}$ , and a comparison of deduced level energies in  $^{23}\text{P}$  with previous results. All entries are given in the c.m. system as MeV  $\pm$  keV and are preceded by their peak number given in Figs. 1 and 2. Those spaces marked by  $\dots$  represent proton groups predicted to be outside our range of observation, while those marked by X correspond to groups which could be detected, but which were not observed. Peaks in parentheses are assignments of new energy levels in  $^{23}\text{P}$  deduced from the present work.

Proton energies corresponding to decay to the following $^{28}\text{Si}$ states:		Deduced excitation energies in $^{23}\text{P}$			
g.s.	1.779	4.618	Present work <sup>a</sup>	Reference	Adopted level energy
6	2.2059 <sup>b</sup>	$\dots$	$4.9541 \pm 0.5, \frac{5}{2}^+$	11	$4.9541 \pm 0.5$
7	2.5448 <sup>b</sup>	1 0.7659 <sup>b</sup>	$5.2930 \pm 0.5, \frac{7}{2}$	11	$5.2930 \pm 0.5$
10	3.067 $\pm$ 15	3 1.302 $\pm$ 10	5.826 $\pm$ 5	17	5.826 $\pm$ 4
11	3.212 $\pm$ 15	X	5.967 $\pm$ 3, $\frac{3}{2}^+$	18, 19	5.967 $\pm$ 3
12	3.326 $\pm$ 15	X	[6.107, ( $\frac{3}{2}^+, \frac{5}{2}$ )] <sup>c</sup>	19, 20	(6.074 $\pm$ 15)
14	3.579 $\pm$ 15	X	6.330 $\pm$ 4, $\frac{3}{2}^+$	18, 19	6.330 $\pm$ 4
X	X	4 1.829 $\pm$ 15	$\dots$		(6.356 $\pm$ 15)
X	X	5 1.978 $\pm$ 15	(6.49); [6.497, ( $\frac{3}{2}^+, \frac{5}{2}$ )] <sup>c</sup>	19, 20	6.505 $\pm$ 15
17	3.905 $\pm$ 15	X	[6.711, ( $\frac{3}{2}^+, \frac{5}{2}$ )] <sup>c</sup>	19, 20	(6.653 $\pm$ 15)
19	4.335 $\pm$ 20	X	[7.070, ( $\frac{3}{2}^+, \frac{7}{2}$ )] <sup>c</sup>	19, 20	(7.083 $\pm$ 20)
X	X	8 2.621 $\pm$ 10	$\dots$		(7.148 $\pm$ 10)
20	4.493 $\pm$ 20	X	7.241 $\pm$ 20	19	7.241 $\pm$ 20
21	4.640 $\pm$ 25	X	7.362 $\pm$ 10	19	7.366 $\pm$ 9
X	X	9 2.986 $\pm$ 15	7.527 $\pm$ 5, ( $\leq \frac{5}{2}^+, \frac{1}{2}$ ) <sup>-</sup>	18, 19	7.526 $\pm$ 5
23	5.008 $\pm$ 20	X	7.759 $\pm$ 5, ( $\frac{3}{2}^+$ )	18, 19	7.759 $\pm$ 5
24	5.359 $\pm$ 15	X	8.105 $\pm$ 11, $\frac{3}{2}^+$	13, 19	8.106 $\pm$ 9
25	5.493 $\pm$ 15	15 3.715 $\pm$ 15	8.221 $\pm$ 11, ( $\frac{3}{2}^+, \frac{5}{2}$ ) <sup>+</sup>	13, 19	8.231 $\pm$ 11 <sup>d</sup>
26	5.6324 <sup>b</sup>	16 3.8535 <sup>b</sup>	8.3806 $\pm$ 2.1, $\frac{5}{2}^+, T = \frac{3}{2}$	12-16	8.3806 $\pm$ 2.1
27	5.784 $\pm$ 20	18 4.008 $\pm$ 20	8.530 $\pm$ 11, ( $\frac{3}{2}^+, \frac{5}{2}$ ) <sup>+</sup>	13, 19	8.532 $\pm$ 9
28	6.062 $\pm$ 30	X	8.781 $\pm$ 15	19	8.787 $\pm$ 13
29	6.676 $\pm$ 30	22 4.852 $\pm$ 20	9.389 $\pm$ 15	19	9.390 $\pm$ 12
$\dots$	Unassigned proton peak				
13	3.414 $\pm$ 15				
			g.s. -6.162 $\pm$ 15		
			1x -7.941 $\pm$ 15		

<sup>a</sup>Excitation energies have been calculated from the present work or recalculated from previous work using a proton separation energy of  $2.7482 \pm 0.0008$  MeV.

<sup>b</sup>These proton energies were used, in part, to determine the energy calibration.

<sup>c</sup>The level energy and  $J^\pi$  values given are those of  $^{23}\text{Si}$  (Refs. 19, 20), the mirror nucleus of  $^{23}\text{P}$ .

<sup>d</sup>This error bar has been increased slightly by a scaling factor,  $S = [\chi^2/(n-1)]^{1/2}$ , to better represent the real uncertainty in the final number.

well with the previous measurements<sup>3,4</sup> of  $195 \pm 8$  and  $180 \pm 10$  ms. The weighted average of these three measurements is  $188.0 \pm 4.3$  ms. This value has been adopted for all subsequent calculations and results quoted herein.

#### IV. ANALYSIS

##### A. Level assignments

The straightforward assignment of the observed proton groups to specific levels in  $^{29}\text{P}$  is complicated by the fact that two possible proton decay channels are available for states with excitation energies greater than 4.5 MeV. Thus the level assignments given in Table I are supported, insofar as possible, through correspondence to known levels in  $^{29}\text{P}$  or in its mirror nucleus,  $^{29}\text{Si}$ . The excitation energies deduced from these assignments are in good agreement with the known excitation energies determined from proton resonance and particle transfer reactions (see Table I).

Recent studies of Detorie *et al.*,<sup>17</sup> utilizing the  $^{32}\text{S}(p, \alpha)$  reaction, have revealed several previously unobserved states in the energy region from 4.6 to 6.0 MeV. One of these new levels at 5.826 MeV has been confirmed in the present study with proton decay of this level to the ground state as well as to the first excited state in the daughter nucleus,  $^{28}\text{Si}$ , being observed. At higher excitation energies, Gearhart *et al.*<sup>18</sup> have made spin and parity assignments for several levels with energies from 6 to 8 MeV using the  $^{28}\text{Si}(p, p'\gamma)$  reaction. Assuming that the spin and parity of  $^{29}\text{S}$  is  $\frac{5}{2}^+$ , to be consistent with the  $J^\pi = \frac{5}{2}^+$  ground state<sup>19</sup> of its mirror,  $^{29}\text{Al}$ , and the assignment of  $J^\pi = \frac{5}{2}^+$  to the lowest  $T = \frac{3}{2}$  state in  $^{29}\text{P}$  (Ref. 19), allowed  $\beta$  decay of  $^{29}\text{S}$  would populate levels in  $^{29}\text{P}$  which have spins and parities of  $\frac{3}{2}^+$ ,  $\frac{5}{2}^+$ , or  $\frac{7}{2}^+$ . Of the four levels with their  $J^\pi$  values determined by Gearhart *et al.*<sup>18</sup> three levels were observed in this work (at  $E_x = 5.967$ , 6.330, and 7.759 MeV) with the fourth level at 6.832 MeV apparently being very weakly fed (see upper limit given in Table II). Decay of the state at 6.330 MeV, giving rise to group 14, was observed to have a line width of  $70 \pm 30$  keV (once the experimental resolution had been subtracted), consistent with the known level width<sup>18,19</sup> of  $73 \pm 5$  keV. (All other strong groups had level widths less than 60 keV, while no reliable widths could be extracted for the weaker groups.) Several states with excitation energies above 8 MeV have been observed to emit delayed protons in agreement with  $^{28}\text{Si}(p, p)$  and  $^{28}\text{Si}(p, p')$  results.<sup>13,19</sup>

Three proton groups (12, 17, and 19) have been tentatively assigned to three previously unobserved

states in  $^{29}\text{P}$  through comparison with known<sup>19,20</sup> levels of appropriate spin and parity in the mirror nucleus,  $^{29}\text{Si}$  [ $E_x = 6.107$  MeV,  $J^\pi = (\frac{3}{2}^+, \frac{5}{2})$ ;  $E_x = 6.711$  MeV,  $J^\pi = (\frac{3}{2}^+, \frac{5}{2}^+)$ ;  $E_x = 7.070$  MeV,  $J^\pi = (\frac{3}{2}^+, \frac{7}{2})$ ]. Since level to level agreement between mirror states (with  $\beta$ -allowed  $J^\pi$  values) of  $^{29}\text{P}$  and  $^{29}\text{Si}$  exists up to an excitation energy of 5.5 MeV, the possibility of additional levels which could be populated by allowed  $\beta$  transitions in this energy region is unlikely. With this noted, assignments of proton groups 4 and 8 to previously unobserved levels at 6.356 and 7.148 MeV, respectively, are proposed; these states then decay predominantly to the first excited state of  $^{28}\text{Si}$  rather than to its ground state. Group 13 has been left unassigned due to the lack of supplementary information needed to determine which final state in  $^{28}\text{Si}$  was populated; however, its intensity has been included in the subsequent branching ratio calculations.

Relative intensities were determined from each group by comparing the number of integrated counts observed in each proton peak. Decomposition of multiplets was accomplished using a Gaussian peak-fitting program. The fraction of the total proton decays for each level are given in the third column of Table II. For those  $T = \frac{1}{2}$  levels which emit protons to both the ground state and first excited state in  $^{28}\text{Si}$ , their relative intensities and reduced width ratios are given in Table III.

Three proton groups arising from the decay of the lowest  $T = \frac{3}{2}$  state in  $^{29}\text{P}$  have been observed. Their intensities and proton branching ratios are given in Table IV. The energetically allowed proton decay of this state to the third excited state of  $^{28}\text{Si}$  was not observed. On the basis of penetrability calculations *alone*, the proton branch to this state is estimated to be five orders of magnitude smaller than that for decay to the ground state. An upper limit on the strength for decay to this state has been determined from our data (see Table IV), but has *not* been included in the branching ratios and  $\log ft$  calculations which follow.

##### B. Branching ratios and $\log ft$ values

The proton intensities are directly related to the preceding  $\beta$ -decay transition rates since  $\gamma$  decay does not compete favorably with proton decay for states which are unbound by more than  $\sim 500$  keV. Even in an unfavorable case such as the decay of the  $T = \frac{3}{2}$  state in  $^{29}\text{P}$ , whose proton decay is isospin forbidden, the partial  $\gamma$  decay width is 0.8 eV (using the results from Ref. 12 and our ratio of  $\Gamma_{P_0}/\Gamma$ ) compared to the total width of 360 eV.<sup>21</sup> Since the absolute branching ratio to the analog state can be calculated nearly model independently, as shown below, absolute branching

TABLE II. Branching ratios and  $\log ft$  values for the positron decay of  $^{29}\text{S}$  compared to shell model calculations.

Energy level in $^{29}\text{P}^a$ (MeV)	$J^\pi$	Proportion of proton decays (%)	Branching ratio from $^{29}\text{S}^b$ (%)	$\log ft^b$ (sec)	Theoretical predictions $^c$		
					$\log ft$ (sec)	$J^\pi$	$E_x$ in $^{29}\text{P}$ (MeV)
0.000	$\frac{1}{2}^+$		$<6 \times 10^{-5}$	$>11.0^d$		$\frac{1}{2}^+$	0.00
1.383	$\frac{3}{2}^+$		$27.2 \pm 2.1^e$	$5.07 \pm 0.03$	4.77	$\frac{3}{2}^+$	1.88
1.954	$\frac{5}{2}^+$		$4.5 \pm 0.4^e$	$5.74 \pm 0.04$	5.46	$\frac{5}{2}^+$	2.62
2.423	$\frac{3}{2}^+$		$20.7 \pm 1.9^e$	$4.99 \pm 0.04$	4.63	$\frac{3}{2}^+$	3.64
3.106	$\frac{5}{2}^+$		$0.9 \pm 0.3^e$	$6.21 \pm 0.15$	7.28	$\frac{5}{2}^+$	4.48
4.080	$\frac{7}{2}^+$	$<1.1$	$<0.5$	$>6.2$	7.18	$\frac{7}{2}^+$	5.39
4.954	$\frac{5}{2}^+$	$25.5 \pm 0.6$	$11.9 \pm 0.4$	$4.65 \pm 0.02$	4.44	$\frac{5}{2}^+$	6.14
5.293	$\frac{7}{2}^+$	$8.4 \pm 0.7$	$3.9 \pm 0.3$	$5.04 \pm 0.04$	4.47	$\frac{7}{2}^+$	6.67
5.826		$8.6 \pm 0.9$	$4.0 \pm 0.4$	$4.88 \pm 0.05$	4.92	$\frac{7}{2}^+$	7.07
5.967	$\frac{3}{2}^+$	$0.40 \pm 0.05$	$0.18 \pm 0.02$	$6.17 \pm 0.06$	5.43	$\frac{3}{2}^+$	7.56
(6.074)		$0.34 \pm 0.05$	$0.16 \pm 0.02$	$6.20 \pm 0.07$	6.84	$\frac{5}{2}^+$	7.86
6.330	$\frac{3}{2}^+$	$1.71 \pm 0.13$	$0.80 \pm 0.06$	$5.42 \pm 0.04$	5.47	$\frac{3}{2}^+$	7.92
(6.356)		$0.81 \pm 0.10$	$0.38 \pm 0.05$	$5.74 \pm 0.06$	6.74	$\frac{7}{2}^+$	7.98
6.505		$0.65 \pm 0.08$	$0.30 \pm 0.04$	$5.79 \pm 0.05$	6.08	$\frac{3}{2}^+$	8.27
(6.653)		$1.53 \pm 0.13$	$0.71 \pm 0.06$	$5.37 \pm 0.04$	5.28	$\frac{7}{2}^+$	8.41
6.832 $^f$	$\frac{5}{2}^+$	$<0.7$	$<0.3$	$>5.7$	6.09	$\frac{5}{2}^+$	8.43
(7.083)		$0.55 \pm 0.06$	$0.26 \pm 0.03$	$5.66 \pm 0.05$	4.30	$\frac{5}{2}^+$	8.59
(7.148)		$2.31 \pm 0.13$	$1.08 \pm 0.07$	$5.02 \pm 0.03$	5.54	$\frac{7}{2}^+$	8.90
7.241		$0.72 \pm 0.08$	$0.33 \pm 0.04$	$5.49 \pm 0.05$	5.28	$\frac{5}{2}^+$	9.05
7.366		$0.53 \pm 0.08$	$0.25 \pm 0.04$	$5.58 \pm 0.07$	8.23	$\frac{3}{2}^+$	9.34
7.526	$(\frac{3}{2}^+, \frac{5}{2}^+)$	$0.18 \pm 0.03$	$0.082 \pm 0.015$	$5.99 \pm 0.08$	5.73	$\frac{7}{2}^+$	9.50
7.759	$(\frac{3}{2}^+)$	$0.49 \pm 0.08$	$0.23 \pm 0.04$	$5.46 \pm 0.07$	5.69	$\frac{5}{2}^+$	9.64
8.106	$\frac{5}{2}^+$	$1.48 \pm 0.15$	$0.69 \pm 0.07$	$4.83 \pm 0.05$	5.73	$\frac{3}{2}^+$	9.69
8.231	$(\frac{3}{2}^+, \frac{5}{2}^+)$	$2.17 \pm 0.30$	$1.01 \pm 0.14$	$4.61 \pm 0.06$	5.70	$\frac{7}{2}^+$	9.97
8.381	$\frac{5}{2}^+, T = \frac{3}{2}$	$39.2 \pm 0.9$	$18.3 \pm 0.6$	3.29	3.29	$\frac{5}{2}^+, T = \frac{3}{2}$	8.86
8.532	$(\frac{3}{2}^+, \frac{5}{2}^+)$	$2.44 \pm 0.20$	$1.14 \pm 0.10$	$4.43 \pm 0.04$	5.74	$\frac{5}{2}^+$	10.01
8.787		$0.31 \pm 0.06$	$0.14 \pm 0.03$	$5.20 \pm 0.09$	6.25	$\frac{3}{2}^+$	10.10
9.390		$0.92 \pm 0.10$	$0.43 \pm 0.05$	$4.40 \pm 0.12$	6.34	$\frac{5}{2}^+$	10.15
$E_p = 3.414^g$		$0.73 \pm 0.06$	$0.34 \pm 0.03$				

<sup>a</sup>Energies below 5.5 MeV have been taken from Ref. 11, while energies for states at higher excitation are taken from Table I.

<sup>b</sup>The branching ratios and  $\log ft$  values are calculated assuming complete isospin purity of the  $T = \frac{3}{2}$  state at 8.381 MeV (see text). An allowance has been made for the 0.22%  $\gamma$ -decay branch from this state (Refs. 12 and 21).

<sup>c</sup>Reference 2.

<sup>d</sup> $\log ft$  limit for second forbidden decay to ground state adopted from Ref. 31.

<sup>e</sup>These branching ratios were calculated from comparison to the mirror  $^{29}\text{Al}$  decay (Ref. 19).

<sup>f</sup>Reference 18.

<sup>g</sup>This unassigned peak is discussed in the text.

TABLE III. Proton branching ratios and reduced widths for  $T = \frac{1}{2}$  states in  $^{29}\text{P}$ .

$E_x$ in $^{29}\text{P}$ (MeV)	Intensities <sup>a</sup> for proton decay to		Reduced width ratio <sup>b</sup>	
	g.s.	1.779 MeV	$\gamma_{p}^2(1.779)/\gamma_{p}^2$ $\frac{3^+}{2}, \frac{5^+}{2}$	$\gamma_{p}^2(1.779)/\gamma_{p}^2$ $\frac{1^+}{2}$ (g.s.)
5.293	1.14 ± 0.09	7.3 ± 0.7	(250) <sup>c</sup>	70
5.826	0.39 ± 0.05	8.2 ± 0.9	70	17
8.231	1.96 ± 0.30	0.21 ± 0.04	0.080	(0.015) <sup>c</sup>
8.532	1.87 ± 0.15	0.57 ± 0.13	0.22	(0.04) <sup>c</sup>
9.390	0.34 ± 0.06	0.58 ± 0.08	1.20	0.27

<sup>a</sup>These intensities are quoted as the percentage of the total proton decays from  $^{29}\text{P}$ .

<sup>b</sup>The reduced width ratios are obtained by dividing the observed intensity by its respective penetrability factor, assuming the state has  $J^\pi = \frac{3^+}{2}, \frac{5^+}{2},$  or  $\frac{1^+}{2}$  [i.e.,  $\gamma_p^2(1.779)/\gamma_p^2(\text{g.s.}) = [I(1.779)/I(\text{g.s.})]/[P(1.779)/P(\text{g.s.})]$ . The penetrabilities were calculated using  $P = kR/(F_L^2 + G_L^2)$  where  $F_L$  and  $G_L$  are the regular and irregular Coulomb functions and  $L$  is the lowest allowed angular momentum of the emitted proton. This expression was evaluated using an interaction radius,  $R = 5.3$  fm.

<sup>c</sup>Since the  $J^\pi$  of these states are known, these have been given for comparison purposes only.

ratios have been obtained by comparing the observed proton intensity for each level with the proton intensity observed for the decay of the analog state (a minor correction to account for the small  $\gamma$ -decay branch has been included).

The Fermi matrix element connecting members of the same isobaric multiplet (with isospin  $T$  and initial/final isospin projection,  $T_{z_i}/T_{z_f}$ ) is given by

$$\langle 1 \rangle^2 = T(T+1) - T_{z_i}T_{z_f}, \quad (1)$$

thus in the present case of superallowed  $\beta$  decay of  $^{29}\text{S}$ ,  $\langle 1 \rangle^2 = 3$ . Unfortunately, the Gamow-Teller matrix element cannot be expressed so simply since it depends on the inherent details of the wave functions, and hence its evaluation is dependent upon the nuclear model used to describe the

initial and final states. Recent shell-model calculations of Chung and Wildenthal<sup>2</sup> predict a value of  $\langle \sigma \rangle^2 = 0.10$ , while an earlier estimate<sup>22</sup> using the Nilsson formalism gave  $\langle \sigma \rangle^2 = 0.24$ . However, owing to the magnitude of the Fermi contribution, uncertainties of this order in  $\langle \sigma \rangle^2$  change the  $ft$  value by only 7% and the  $\log ft$  by only 0.03. Thus the superallowed transition rate can be calculated nearly model independently. In this work a  $\log ft = 3.29$ , as predicted<sup>2</sup> using the shell model, has been utilized to estimate the absolute branching ratio to the lowest  $T = \frac{3}{2}$  state in  $^{29}\text{P}$ . The corresponding branching ratios to the remaining unbound levels have been determined through a comparison of proton intensities (see column 4 of Table II).

Branching ratios to the proton bound levels were then calculated from the mirror  $^{29}\text{Al} \leftrightarrow ^{29}\text{Si}^*$  transition rates<sup>19</sup> which have been renormalized slightly to account for the missing strength. The resulting asymmetry between  $\beta^+$ - and  $\beta^-$ -decay transition rates of  $(ft)^+/(ft)^- = 1.04 \pm 0.07$  indicates good overall mirror symmetry averaging over the first four excited states.  $\beta^+$  decay of  $^{29}\text{S}$  to the ground state of  $^{29}\text{P}$  is second forbidden so that branching to the ground state is strongly hindered (see upper limit given in Table II). The partial half-lives for each transition have been determined from the branching ratios using the measured half-life of  $^{29}\text{S}$ ; after multiplication by  $f$ , the statistical rate function whose evaluation is discussed below, the final  $ft$  value for each transition was obtained. The experimental  $\log ft$  values are presented in column 5 of Table II, as well as in the decay scheme shown in Fig. 3.

The statistical rate function was calculated using the method of Bahcall<sup>23</sup> which takes into account nuclear screening from atomic electrons. Furthermore, radiative corrections<sup>24,25</sup> and corrections due to finite nuclear size<sup>26</sup> have also been included in these calculations.

TABLE IV. Proton decay of the lowest  $T = \frac{3}{2}$  state in  $^{29}\text{P}$ .

Final state in $^{29}\text{Si}$ <sup>a</sup> (MeV)	Proton energy <sup>b</sup> (MeV)	Observed intensity <sup>c</sup> $I$ (%)	Relative branching ratio (%)	Penetrability $P$ <sup>d</sup>	$I/P$ <sup>e</sup>
0.000	0 <sup>+</sup>	5.632	33.9 ± 0.8	0.74	0.46
1.779	2 <sup>+</sup>	3.854	5.00 ± 0.25	1.05	0.048
4.618	4 <sup>+</sup>	1.015	0.34 ± 0.13	$2.8 \times 10^{-4}$	12
4.979	0 <sup>+</sup>	0.653	<1.1	$7.9 \times 10^{-6}$	<1400

<sup>a</sup>Reference 19.

<sup>b</sup>These energies are expressed in the c.m. system.

<sup>c</sup>As percent of total proton decay.

<sup>d</sup>These penetrabilities were calculated in the manner discussed in Table III.

<sup>e</sup> $I/P$  is the observed intensity (column 4) divided by its penetrability (column 6).

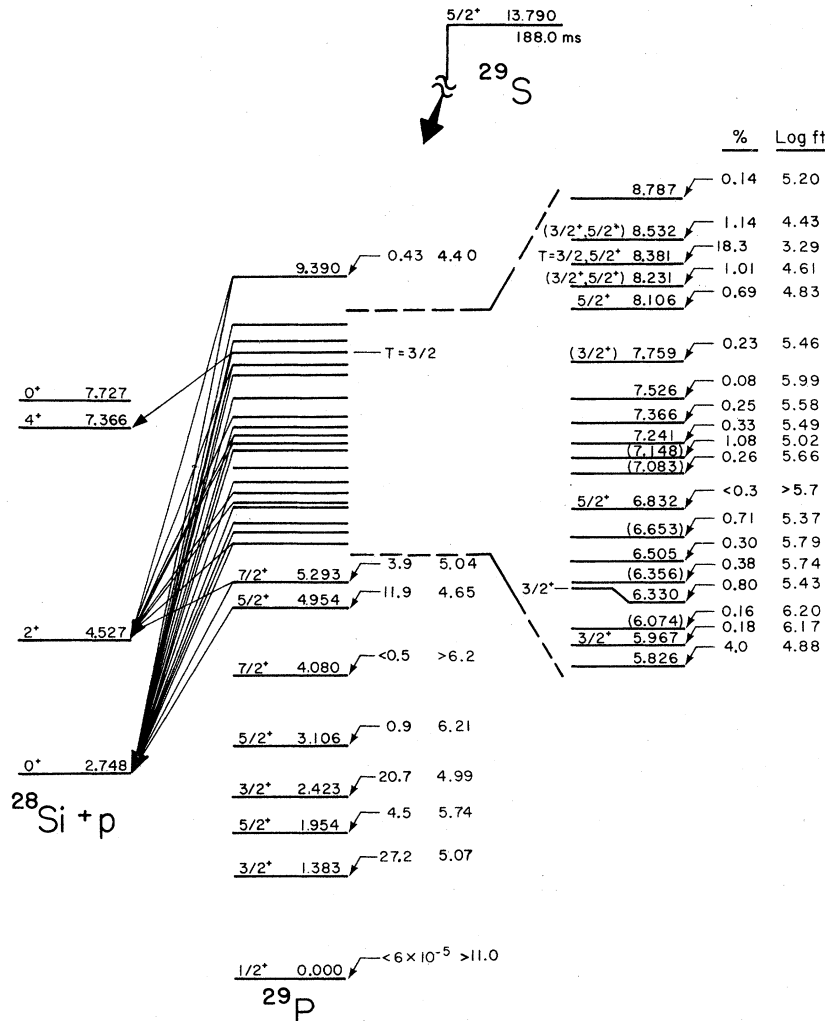


FIG. 3. Proposed decay scheme for  $^{29}\text{S}$ . Absolute branching ratios and log  $ft$  values are indicated (see text).

## V. DISCUSSION AND CONCLUSION

Comparison between the experimental results and the theoretical predictions of Chung and Wildenthal<sup>2</sup> are given in Table II and illustrated in Fig. 4. These shell-model calculations employ *their interaction*<sup>27</sup> which has been fitted to the energy levels of nuclei with mass 18 to 24. Since the  $A = 29$  system is located near the middle of the  $2s1d$  shell, where matrix dimensions are maximal, a truncated basis space, restricted to 6 or more particles in the  $1d_{5/2}$  subshell, was employed in these calculations.

Correlation of levels up to an excitation energy of 6 MeV indicated that the level order has been correctly predicted, although the theoretical excitation energies are 0.5 to 1.4 MeV higher than is experimentally observed. To some extent this discrepancy results from basis space truncation

since, in an additional calculation employing the full  $2s1d$  shell space, the binding energy of the  $J^\pi = \frac{1}{2}^+$  ground state increased by 0.6 MeV compared to the truncated basis prediction; shifts for excited states are expected to be larger.<sup>2</sup> Similar shifts in predicted level energies employing complete or truncated  $2s1d$  shell model spaces were also found in the  $A = 29$  calculations of Cole *et al.*<sup>28</sup> for several states with  $J^\pi \geq \frac{5}{2}^+$ .

Of the nine levels correlated, good agreement between predicted and observed  $\beta^+$ -decay transition rates was found. Less than a 10% difference in log  $ft$  values was observed between theory and experiment, excluding the highly hindered transition to the level at 3.106 MeV, whose discrepancy represents only a small absolute change in the Gamow-Teller matrix element arising from subtle details in the wave functions. Although the  $\frac{7}{2}^+$  state at 4.080 MeV is well above the proton





increase in level density and the lack of spin and parity information. After normalizing the shell-model calculations to the state at 4.954 MeV (see Fig. 4) to offset the energy difference noted earlier, 21 levels with  $J^\pi = \frac{3}{2}^+$ ,  $\frac{5}{2}^+$ , or  $\frac{7}{2}^+$  are predicted to lie above the proton separation energy in  $^{29}\text{P}$  and be fed with at least a 0.1% absolute branch, while 20 levels with similar branching were observed with one group remaining unassigned. The predicted strength to levels with excitation energies of 4.0 to 9.5 MeV constitutes a summed branching strength of 45% in good agreement with the observed summed strength of 47%.

Using the spin and parity guidelines of Raman and Gove,<sup>31</sup> those transitions which have  $\log ft$  values less than 5.9 are restricted to spins and parities consistent with allowed  $\beta$  decay. Our data then agree with all of the previous spin and parity determinations or limits imposed by  $\gamma$  decay and reaction studies (see Table I) and restrict the parity of the 5.293 MeV state to being positive (i.e.,  $J^\pi = \frac{7}{2}^+$ ). Our result for the decay to the 7.526 MeV state is marginally above this limit but supports the earlier tentative assignment of  $J^\pi \leq \frac{5}{2}^+$  (Ref. 19) for this state rather than the tentative assignment of  $\frac{1}{2}^-$  given by Gearhart *et al.*<sup>18</sup>

Enhanced transition strengths to states at 8.106, 8.231, and 8.532 MeV, surrounding the 8.381 MeV,  $T = \frac{3}{2}$  state (IAS), are observed. Since the 8.106

MeV state is believed to have  $J^\pi = \frac{5}{2}^+$  and the other two states have possible  $J^\pi = \frac{5}{2}^+$ , it is interesting to consider whether these enhancements are the result of isospin mixing with the IAS ( $J^\pi = \frac{5}{2}^+$ ). Taking a value for a typical Gamow-Teller contribution of  $\langle\sigma\rangle = 0.20$ , which results in a  $\log ft = 5.0$ , these enhancements could be explained by mixing with the IAS of 1–6% for each level, resulting in an isospin purity of ~90% for the IAS. This would be consistent with the isospin purity measured for other members of this series, in particular  $^{17}\text{Ne}$ :  $\geq 95\%$  (Ref. 32),  $^{33}\text{Ar}$ :  $81 \pm 9\%$  (Ref. 32), and  $^{41}\text{Ti}$ :  $91 \pm 4\%$  (Ref. 33). Alternatively, the enhanced  $\beta$  strength might be explained by a collective Gamow-Teller transition as predicted in the gross theory of  $\beta$  decay.<sup>34,35</sup> Determining the true source of the enhanced  $\beta$  strength which is observed surrounding many of the analog states in this series of  $\beta$ -delayed proton precursors poses a most intriguing and fundamental problem.

We would like to thank W. Chung and B. H. Wildenthal for supplying these shell-model calculations prior to publication and for several helpful discussions concerning these calculations. This work was supported by the Nuclear Physics and Nuclear Sciences Divisions of the Department of Energy.

<sup>1</sup>J. Cerny and J. C. Hardy, *Ann. Rev. Nucl. Sci.* **27**, 333 (1977); J. C. Hardy, in *Nuclear Spectroscopy and Reactions—Part C*, edited by J. Cerny (Academic, New York, 1974), p. 417.

<sup>2</sup>W. Chung and B. H. Wildenthal, private communication.

<sup>3</sup>J. C. Hardy and R. I. Verrall, *Phys. Lett.* **13**, 148 (1964); R. I. Verrall, McGill University, Ph.D. thesis, 1968 (unpublished).

<sup>4</sup>R. W. Fink, T. H. Braid, and A. M. Friedman, *Ark. Fys.* **36**, 471 (1967).

<sup>5</sup>R. G. Sextro, R. A. Gough, and J. Cerny, *Phys. Rev. C* **8**, 258 (1973).

<sup>6</sup>R. G. Sextro, University of California, Ph.D. thesis, 1973, Lawrence Berkeley Laboratory Report No. LBL-2360 (unpublished).

<sup>7</sup>R. D. Macfarlane and William McHarris, in *Nuclear Spectroscopy and Reactions—Part A*, edited by J. Cerny (Academic, New York, 1974), p. 243; W. Weisehahn, G. Bischoff, and J. D'Auria, *Nucl. Instrum. Methods* **129**, 187 (1975) and references therein.

<sup>8</sup>A. H. Wapstra and K. Bos, *At. Data and Nucl. Data Tables* **19**, 177 (1977).

<sup>9</sup>D. J. Vieira, D. F. Sherman, M. S. Zisman, R. A. Gough, and J. Cerny, *Phys. Lett.* **60B**, 261 (1976).

<sup>10</sup>D. J. Vieira, University of California, Ph.D. thesis, 1978, Lawrence Berkeley Laboratory Report No. LBL-7161 (unpublished).

<sup>11</sup>T. Byrski, F. A. Beck, P. Engelstein, M. Forterre, and A. Knipper, *Nucl. Phys.* **A223**, 125 (1974).

<sup>12</sup>D. H. Youngblood, G. C. Morrison, and R. E. Segel, *Phys. Lett.* **22**, 625 (1966).

<sup>13</sup>B. Teitelman and G. M. Temmer, *Phys. Rev.* **177**, 1656 (1969).

<sup>14</sup>G. C. Morrison, D. H. Youngblood, and R. C. Bearse, *Phys. Rev.* **174**, 1366 (1968).

<sup>15</sup>T. T. Bardin, J. A. Becker, and T. R. Fisher, *Phys. Rev. C* **5**, 1351 (1972).

<sup>16</sup>R. A. Gough, R. G. Sextro, and J. Cerny, *Phys. Lett.* **43B**, 33 (1973).

<sup>17</sup>N. A. Detorie, J. D. Goss, A. A. Rollefson, and C. P. Browne, *Phys. Rev. C* **10**, 991 (1974).

<sup>18</sup>N. L. Gearhart, H. J. Hausman, J. F. Morgan, G. A. Norton, and N. Tsoupas, *Phys. Rev. C* **10**, 1739 (1974); N. Tsoupas, H. J. Hausman, N. L. Gearhart, and G. H. Terry, *ibid.* **13**, 510 (1976).

<sup>19</sup>P. M. Endt and C. Van der Leun, *Nucl. Phys.* **A214**, 1 (1973).

<sup>20</sup>D. A. Viggars, P. A. Butler, P. E. Carr, L. L. Gadenken, L. L. Green, A. N. James, P. J. Nolan, and J. F. Sharpey-Schafer, *J. Phys. A: Math., Nucl. Gen.* **7**, 360 (1974).

<sup>21</sup>P. G. Kossi, T. B. Clegg, W. W. Jacobs, E. J. Ludwig, and W. J. Thompson, *Nucl. Phys.* **A274**, 1 (1976).

<sup>22</sup>J. C. Hardy and B. Margolis, *Phys. Lett.* **15**, 276 (1965).

<sup>23</sup>J. N. Bahcall, *Nucl. Phys.* **75**, 10 (1966).

<sup>24</sup>D. H. Wilkinson and B. E. F. Macefield, *Nucl. Phys.* **A158**, 110 (1970).

- <sup>25</sup>W. Jaus and G. Rasche, Nucl. Phys. A143, 202 (1970).
- <sup>26</sup>D. H. Wilkinson, Nucl. Phys. A158, 476 (1970).
- <sup>27</sup>W. Chung, Michigan State University, Ph.D. thesis, 1977 (unpublished); W. Chung and B. H. Wildenthal (unpublished).
- <sup>28</sup>B. J. Cole, A. Watt, and R. R. Whitehead, J. Phys. G: Nucl. Phys. 1, 935 (1975).
- <sup>29</sup>L. Meyer-Schützmeister, D. S. Gemmell, R. E. Holland, F. T. Kuchnir, H. Ohnuma, and N. G. Puttaswamy, Phys. Rev. 187, 1210 (1969).
- <sup>30</sup>R. C. Haight, I. D. Proctor, H. F. Lutz, and W. Bartolini, Nucl. Phys. A241, 285 (1975).
- <sup>31</sup>S. Raman and N. B. Gove, Phys. Rev. C 7, 1995 (1973).
- <sup>32</sup>J. C. Hardy, J. E. Esterl, R. G. Sextro, and J. Cerny, Phys. Rev. C 3, 700 (1971).
- <sup>33</sup>R. G. Sextro, R. A. Gough, and J. Cerny, Nucl. Phys. A234, 130 (1974).
- <sup>34</sup>K. Takahashi and M. Yamada, Prog. Theor. Phys. 41, 1470 (1969); S. I. Koyama, K. Takahashi, and M. Yamada, *ibid.* 44, 663 (1970); K. Takahashi, M. Yamada, and T. Kondoh, At. Data Nucl. Data Tables 12, 101 (1973).
- <sup>35</sup>J. C. Hardy, Proceedings of the International Conference on Nuclei far from Stability, Cargèse, Corsica, 1976, CERN Report No. 76-13, p. 267 (unpublished).